Hydrogen Sulfide Inhibits Bronchial Epithelial Cell Epithelial Mesenchymal Transition Through Regulating Endoplasm Reticulum Stress

Fan Lin [1,2], Chengcheng Liao [1], Jinsheng Zhang [3], Yun Sun [1], Weiwei Lu [3], Yu Bai [1], Yixuan Liao [1], Minxia Li [1], Yongfen Qi [3]* and Yahong Chen [1]*

[1]Department of Respiratory and Critical Care Medicine, Peking University Third Hospital, Beijing, China, [2]Geriatric Medicine Center, Department of Pulmonary and Critical Care Medicine, Zhejiang Provincial People's Hospital (Affiliated People's Hospital, Hangzhou Medical College), Hangzhou, China, [3]Key Laboratory of Molecular Cardiovascular Science, Ministry of Education, Peking University Health Science Center, Beijing, China

Epithelial mesenchymal transition (EMT) is a contributing factor in remodeling events of chronic obstructive pulmonary disease (COPD). Hydrogen sulfide (H_2S) has been implicated in the pathogenesis of COPD, but the effect of H_2S in regulating EMT and the underlying mechanisms is not clear. In this study, we assessed endoplasmic reticulum (ER) stress markers, EMT markers and associated signal molecules in rat lungs, bronchial epithelial cells, and human peripheral lung tissues to investigate the effect of H_2S in regulating EMT and the underlying mechanisms. We found that EMT and ER stress occurred in lung epithelial cells, especially in the bronchial epithelial cells of smokers and COPD patients. In cigarette smoke (CS)-exposed rats, intraperitoneal injection of NaHS significantly alleviated CS-induced lung tissue damage, small airway fibrosis, ER stress, and EMT, while intraperitoneal injection of propargylglycine (cystathionine-gamma-lyase inhibitor) aggravated these effects induced by CS. In the nicotine-exposed 16HBE cells, an appropriate concentration of H_2S donor not only inhibited nicotine-induced ER stress, but also inhibited nicotine-induced enhancement of cell migration ability and EMT. ER stress nonspecific inhibitors taurine and 4-phenyl butyric acid also inhibited nicotine-induced enhancement of cell migration ability and EMT. Both H2S and inositol-requiring enzyme 1 (IRE1) activation inhibitor 4μ8C inhibited nicotine-induced activation of IRE1, Smad2/3 and EMT. These results suggest that H_2S inhibits CS- or nicotine-induced ER stress and EMT in bronchial epithelial cells and alleviates CS-induced lung tissue damage and small airway

fibrosis. The IRE1 signal pathway and Smad2/3 may be responsible for the inhibitory effect of H$_2$S.

INTRODUCTION

Chronic obstructive pulmonary disease (COPD) has the characteristics of persistent airflow limitation and respiratory symptoms that result from exposure to noxious gases or particles. Among COPD patients, the small airways have the characteristics of epithelial changes, thickening of the small airway wall, inflammatory and mucous exudates induced airway obstruction, inflammatory cell infiltration into the airway wall, proliferation of airway smooth muscle, and progressive peribronchiolar fibrosis (Van den Berge et al., 2011). Small airway dysfunction is an early feature of lung disease and preceded both the detection of emphysema by imaging methods and spirometric evidence of COPD (Hogg et al., 2004). Moreover, there is convincing pathological evidence that a large number of small airways have been lost before the pathological changes of emphysema (Stockley et al., 2017). Small airway remodeling leads to irreversible small airway dysfunction, participating in the pathogenesis of COPD. Cigarette smoke (CS) induced epithelial-mesenchymal transition (EMT) is one of the mechanisms involved in small airway remodeling (Nowrin et al., 2014). In addition, more *in vivo* (Sohal et al., 2010; Sohal et al., 2011) and *in vitro* (Liu et al., 2010; Veljkovic et al., 2011; Eurlings et al., 2014) studies showed that CS-induced EMT in lung epithelial cells contributed to tissue remodeling in patients with COPD. There is convincing evidence that endoplasmic reticulum (ER) stress can activate classic Smad, Wnt/β-catenin and Src protein kinase families, thus inducing EMT in alveolar epithelial cells (Tanjore et al., 2011; Zhong et al., 2011; Zhang et al., 2012). In ER, glucose-regulated protein: 78 (GRP78) binds to three transmembrane sensor protein inositol requiring enzyme 1 (IRE1), activating transcription factor-6 (ATF6), and PKR-like ER kinase (PERK), maintaining each in its inactive state (Osorio et al., 2013; Lindholm et al., 2017; Chadwick and Lajoie, 2019). During ER stress, GRP78 is released from IRE1, ATF6 and PERK, so these three transmembrane sensor proteins can assume their activated state (Lin et al., 2008; Tanjore et al., 2012; Marciniak, 2017). P-IRE1 splices the mRNA of x-box binding protein 1 (XBP1) to the mature form sec-XBP1, which can activate a series of genes involved in ER-associated protein degradation or protein folding, thus playing a protective role in ER stress. However, the downstream effects of the phosphorylation of IRE1 include activation of c-Jun N-terminal kinase (JNK), which mediates some of the harmful effects such as proliferation, differentiation, carcinogenesis, or apoptosis (Tabas and Ron, 2011; You et al., 2013). Recent studies also reported that CS induced-ER stress plays a very important role in the occurrence and development of COPD (Alam et al., 2014; Geraghty et al., 2016). This notion was confirmed by findings that ER stress markers significantly correlated with lung function in COPD patients (Min et al., 2011). Nicotine, as an important component of cigarette smoke extract, is directly associated with COPD. Evaluation of electronic nicotine delivery systems in different models has demonstrated involvement in pathways related to chronic pulmonary diseases (Canistro et al., 2017; Singh et al., 2019; Mikheev et al., 2020). Inhaled nicotine induces bronchial epithelial cell apoptosis and senescence *via* reactive oxygen species mediated autophagy impairment in COPD (Bodas et al., 2016). Nicotine can promote EMT in lungs. Maternal nicotine exposure induces EMT in rat offspring lungs (Chen et al., 2015). Nicotine can increase malignancy through EMT in lung cancer (Dasgupta et al., 2009; Pillai et al., 2015; Zhang et al., 2016; Du et al., 2018). Nicotine can directly induce ER stress response (Pelissier-Rota et al., 2015; Barra et al., 2017; Gonzales et al., 2021; Jiang et al., 2021). In our previous study, we confirmed that nicotine concentration and time dependently increased the expression of ER stress associated apoptosis marker in human bronchial epithelial cells (Lin et al., 2017).

Hydrogen sulfide (H$_2$S), known for its poisoning effect, is now recognized as an endogenous gaseous transmitter in health and disease (Wang, 2002). H$_2$S is involved in regulating the tension in airway smooth muscle and has anti-oxidation, anti-inflammation, and anti-apoptosis effects in COPD (Suzuki et al., 2021). According to our previous research, exogenous administration of H$_2$S protected against CS-induced bronchial epithelial cell apoptosis through inhibiting ER stress (Lin et al., 2017). H$_2$S may play a protective role in bronchial epithelial cells through regulating ER stress. Recent research reported that H$_2$S can inhibit EMT and oxidative stress, thus preventing the airway remodeling induced by CS in mouse lungs. H$_2$S can also attenuate CS-induced EMT by inhibiting the activation of the transforming growth factor β1 (TGF-β1) -Smad3 signaling pathway (Guan et al., 2020). Furthermore, Fang LP found that exogenous administration of H$_2$S suppressed TGF-β1 mediated EMT and preincubation with H$_2$S decreased the phosphorylation of Smad2/3 induced by TGF-β1 in human lung carcinoma (A549) cells (Fang et al., 2010). Our previous research found that exogenous H$_2$S could also inhibit TGF-β1 induced human bronchial epithelial cell morphological changes and EMT (Liao et al., 2015). All these results suggest that exogenous administration of H$_2$S can inhibit EMT in the lung. H$_2$S is mainly produced by cystathionine-gamma-lyase (CSE) in respiratory organs. Our group has proposed for the first time that CSE expression is decreased in the lungs of smokers and COPD patients compared with nonsmokers (Sun et al., 2015). The effect of endogenous H$_2$S in the lung and its role in the pathogenesis of EMT and airway remodeling induced by CS remains unclear.

We therefore hypothesized that endogenous H$_2$S might inhibit CS-induced EMT in the lung and that H$_2$S might regulate ER

stress to suppress bronchial epithelial cell EMT, which plays an essential role in the small airway fibrosis of COPD. Therefore, we assessed the ER stress and EMT markers in human lung tissues, rat lung tissues from a COPD rat model established by passive CS exposure, and 16HBE cells exposed to nicotine in order to investigate whether H_2S can inhibit EMT of bronchial epithelial cells by regulating ER stress and possible signal pathways.

MATERIALS AND METHODS

Patients

Human peripheral lung tissue samples from 21 patients who underwent thoracic surgery at Peking University Third Hospital from April 2012 to July 2014 were included in this research. The protocol was authorized by Peking University Third Hospital Ethics Committee (IRB00006761-2012029). All participants were fully informed of the purpose and duration of the research and provided written informed consent. The diagnosis of COPD was made according to the GOLD (Global Initiative for Chronic Obstructive Lung Disease) criteria (GOLD, 2009). Subject age, smoking index, height, weight, and the pulmonary function indexes of forced expiratory volume in 1 s (FEV1), forced vital capacity (FVC) % predicted, and FEV1/FVC were listed in **Supplementary Table S1** to describe the clinical features of patients. All the patients were clinically stable for 4 weeks without acute pulmonary infection, had not received any chemotherapy before the study, and did not have metastasis, obstructive atelectasis, other pulmonary diseases, or severe diseases in other systems. All of the human lung tissues were obtained at least 5 cm away from the tumor margin. The pathological examination confirmed that these samples presented lung structure without inflammation or metastasis.

Animal Model

All animal care and experimental protocols were in compliance with the ethical procedures and policies approved by the Animal Care and Use Committee of the National Research Center and the Third Hospital, Peking University Guide for the Care and Use of Laboratory Animals.

Adult male Sprague–Dawley rats were supplied by the Animal Center, Peking University Health Science Center. All rats were housed in groups of 4 to a cage with sufficient oxygen, at a room temperature of 18–25°C and a room humidity of 35–50%. A total of 32 adult male Sprague–Dawley rats, weighing about 200–250 g, were randomly allocated into four groups (each $n = 8$) for treatment: control, CS, propargylglycine (PPG) + CS and NaHS + CS. Except in the control group, the rats in other groups were exposed whole-body to CS generated by 20 commercial unfiltered cigarettes daily. Exposure time was 4 h a day for 7 days a week in the 4 months. The CS group rats intraperitoneally injected with PPG (CSE inhibitor) was considered to the PPG + CS group. Freshly prepared PPG (37.5 mg/kg body weight/day) was intraperitoneally administered 30 min before CS-exposure in the PPG + CS group since the beginning of the third month. The CS group rats intraperitoneally injected with NaHS (H₂S donor) was

considered part of the PPG + CS group. Freshly prepared NaHS (14 μmol/kg body weight/day) was intraperitoneally administered 30 min before CS-exposure in the NaHS + CS group since the beginning of the third month. The control and CS groups comprised rats with an intraperitoneal injection of saline.

Cell Culture and Treatment

The 16HBE14o- (16HBE) human bronchial epithelial cell line was purchased from Shanghai Bogoo Biotechnology Co., Ltd. (China). 16HBE cells were maintained in a complete RPMI1640 growth medium supplemented with 10% fetal bovine serum (Gibco, Waltham, MA, United States), 100 mg/ml streptomycin (Gibco, Waltham, MA, United States), 100 U/ml penicillin (Gibco, Waltham, MA, United States), and 2 mM L-glutamine (Gibco, Waltham, MA, United States) in a humidified atmosphere with 5% CO_2 at 37°C. Cells were starved in serum-free medium for 24 h before drug treatment. Taurine (10 mM), 4-phenyl butyric acid (4PBA) (5 mM), morpholin-4-ium-4-methoxyphenyl-(morpholino)-phosphinodithioate (GYY4137), and NaHS were dissolved in phosphate buffer solution, nicotine, and 4μ8C were prepared in dimethyl sulfoxide (DMSO).
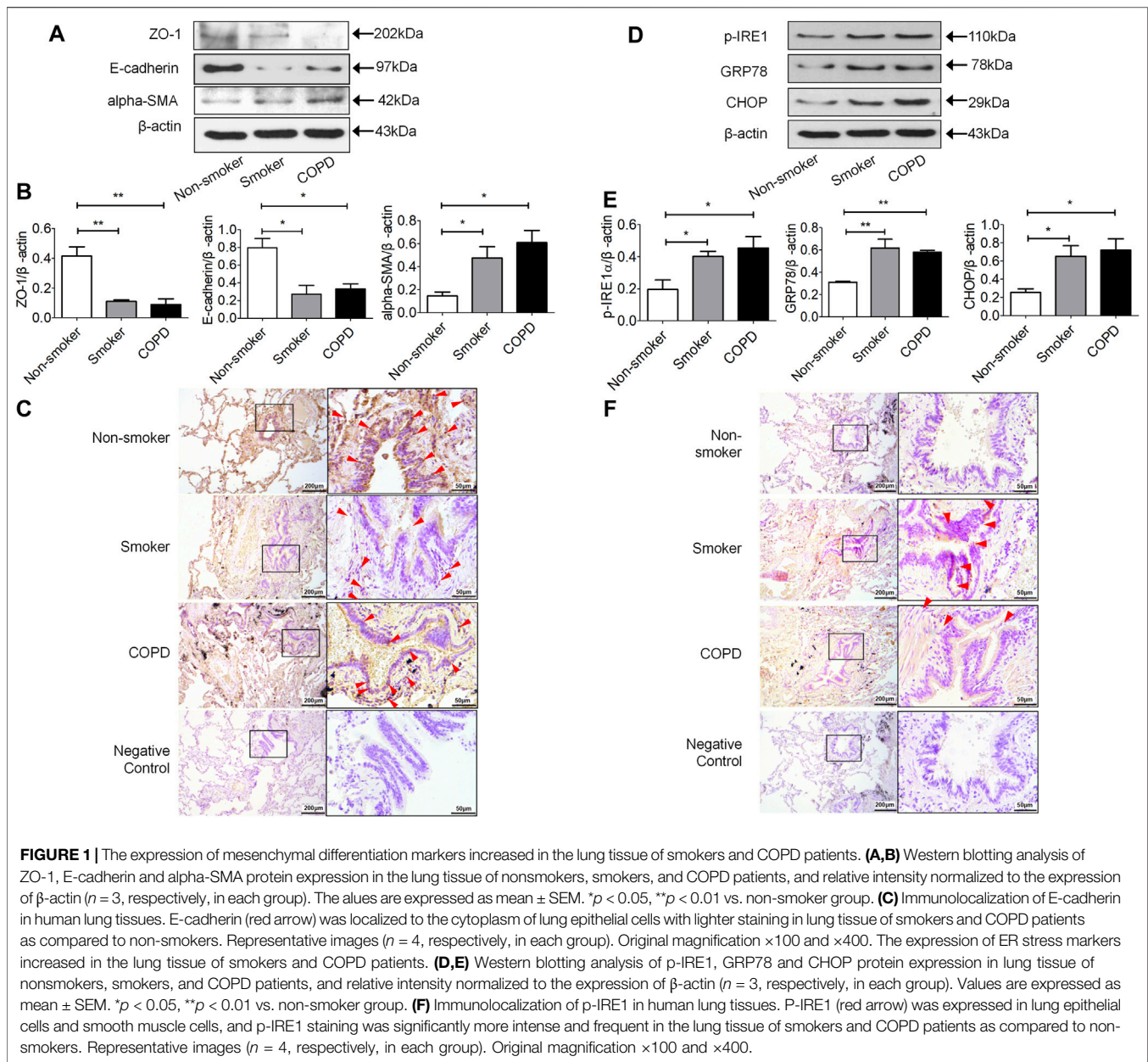
Immunohistochemistry

Lung tissue specimens were fixed in formalin, embedded in paraffin, then cut into 4–6 μm sections and stained with haematoxylin-eosin. The sections were incubated with primary antibodies anti-E-cadherin (1:200), anti-GRP78 (1:200), anti-alpha-smooth muscle actin (alpha-SMA) (1:50), anti-p-IRE1 (1:50) or anti-Vimentin (1:50) at 4°C for 24 h. Anti-goat IgG-conjugated with DAB was used as the secondary antibody at a dilution of 1:100. Pre-immune IgG isotope served as a negative control.

Western Blot Analysis

Protein samples prepared from lung tissue samples and the human bronchial epithelial cell line 16HBE were resolved by SDS-PAGE (10% acrylamide gel) and then transferred to a nitrocellulose membrane. The nitrocellulose membrane was then incubated with the primary antibodies anti-CSE (1:2,000), anti-zonula occludens-1 (ZO-1) (1:1,000), anti-E-cadherin (1:2,000), anti-alpha-SMA (1:500), anti-p-IRE1 (1:1,000), anti-IRE1 (1:1,000), anti-GRP78 (1:3,000), anti-sec-XBP1 (1:500), anti-ATF6 (1:500), anti-p-Smad2/3 (1:500), anti-Smad2/3 (1:500), anti-p-JNK (1:500), anti-JNK (1:500), anti-β-actin (1:3,000) or anti-glyceraldehyde-3-phosphate dehydrogenase (GAPDH) (1:5,000) overnight, then secondary antibody for 1 h. The enhanced chemiluminescence was applied to visualize the reaction. Expression levels of proteins were normalized to those of GAPDH or β-actin.

Hematoxylin and Eosin and Picrosirius Red Staining

The histopathological changes of lung tissue were measured by Hematoxylin and Eosin (HE) staining. The pathological scores of small airways were measured by separate evaluation of eight variables according to Cosio M (Cosio et al., 1978). The airways of 2 mm or less in diameter were measured by the separate

FIGURE 1 | The expression of mesenchymal differentiation markers increased in the lung tissue of smokers and COPD patients. **(A,B)** Western blotting analysis of ZO-1, E-cadherin and alpha-SMA protein expression in the lung tissue of nonsmokers, smokers, and COPD patients, and relative intensity normalized to the expression of β-actin ($n = 3$, respectively, in each group). The alues are expressed as mean ± SEM. *$p < 0.05$, **$p < 0.01$ vs. non-smoker group. **(C)** Immunolocalization of E-cadherin in human lung tissues. E-cadherin (red arrow) was localized to the cytoplasm of lung epithelial cells with lighter staining in lung tissue of smokers and COPD patients as compared to non-smokers. Representative images ($n = 4$, respectively, in each group). Original magnification ×100 and ×400. The expression of ER stress markers increased in the lung tissue of smokers and COPD patients. **(D,E)** Western blotting analysis of p-IRE1, GRP78 and CHOP protein expression in lung tissue of nonsmokers, smokers, and COPD patients, and relative intensity normalized to the expression of β-actin ($n = 3$, respectively, in each group). Values are expressed as mean ± SEM. *$p < 0.05$, **$p < 0.01$ vs. non-smoker group. **(F)** Immunolocalization of p-IRE1 in human lung tissues. P-IRE1 (red arrow) was expressed in lung epithelial cells and smooth muscle cells, and p-IRE1 staining was significantly more intense and frequent in the lung tissue of smokers and COPD patients as compared to non-smokers. Representative images ($n = 4$, respectively, in each group). Original magnification ×100 and ×400.

evaluation of eight variables, including the degree of cell and mucus-induced airway lumen occlusion, which was corrected for lung inflation and expressed as a percent of occluded airway lumen. The presence or absence of mucosal ulcers in small airways was observed and recorded for each airway. The data is shown as a percentage of airways with mucosal ulcers. The remaining variables included squamous-cell metaplasia and goblet-cell metaplasia of the epithelium and changes in the airway wall, which included the amount of connective tissue, muscle, and pigment, and the degree of inflammatory-cell infiltration. Each of these changes was assigned a score ranging from 0 to 3, and these scores were summed to achieve an overall score. Then we expressed the sum as a percent of the maximum possible scores. The final pathological score was

assigned by the simple addition of a score for each of the eight variables in each case.

The collagen deposition in small airways was measured by Picrosirius red staining. The prepared sections were photographed under transmitted or polarized light on a Leica DM IRB fluorescence microscope. Color photographic slides made with tungsten film were converted to digital images by scanning (Wang et al., 2000). By using this technique, loosely packed collagen fibers appear green, whereas tightly packed collagen fibers appear yellow-red and less mature. All these images are then analyzed by Image Pro-plus 6.0 image analysis software. This procedure was applied to a total of five fields per sample on a minimum of four animals per group. All these data were compiled for statistical analyses (Wang et al.,
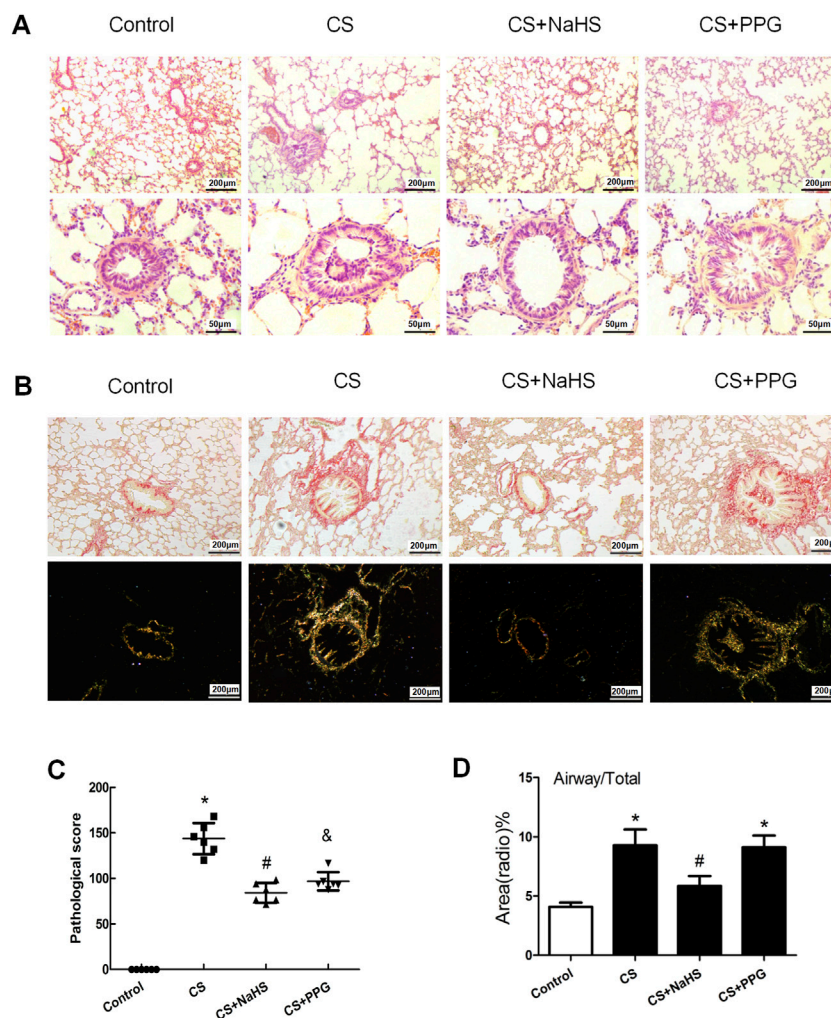
FIGURE 2 | Changes in lung pathology and small airway fibrosis in rats. **(A)** Lung tissue sections were stained with hematoxylin and eosin and examined under light microscopy. Original magnification ×100 and ×400. **(B)** Lung tissue sections were stained with Picrosirius red staining and examined on bright field microscopy (above panels) and polarization microscopy (down panels). Original magnification ×100. **(C)** Airway obstruction, necrotic epithelium, goblet metaplasia, inflammatory cell infiltration, and collagen deposition were seen in the CS group. Emphysema, such as thin or faulted alveolar walls, was seen in the COPD group. Compared with the control group, the pathological score of the small airway was significantly elevated by 42.7% in the CS group ($p < 0.01$), but decreased by 17.9% after NaHS intervention ($p < 0.05$). Results are presented for $n = 8$ mice per group and of 3 independent experiments ($n = 3$, respectively, in each group). *$p < 0.05$, CS group and PPG + CS group vs. Control group. #$p < 0.05$, NaHS + CS group vs. CS group. &$p < 0.05$, PPG + CS group vs. CS group. **(D)** Bar graphs summarizing quantification of small airway fibrosis depended on the Picrosirius red staining and examined on polarization microscopy. Compared with the control group, the collagen deposition around the airway wall was significantly increased in the CS group and the PPG + CS group. The NaHS + CS group had less collagen deposition compared with the CS group. *$p < 0.05$ vs. Control group and #$p < 0.05$ vs. CS group.

2000). The ratio of collagen area to the whole lung tissue area in each image reflected the collagen content.

Wound Healing Assay

The migration ability of human bronchial epithelial cells was measured by a wound healing assay. 16 HBE cells were plated on 60 mm Petri dishes and grew to a confluent monolayer. A single layer of cells was scraped in a straight line with the tip of a sterile pipette (1 ml) on every Petri dish. Then the dishes were washed twice with PBS and replaced with 5 ml of medium containing different drugs. 16 HBE cells were pretreated with NaHS (200 μM) for 0.5 h and then stimulated with nicotine in the Nicotine + NaHS group, and 16 HBE cells were pretreated with taurine (10 mM) for 0.5 h and then stimulated with nicotine in the Nicotine + Taurine group. All the dishes were placed at 37°C for 12 h (Liang et al., 2007). The images were photographed using an inversion fluorescence microscope. Six independent experiments were conducted. The largest migration distance and the closure rate were calculated by IPP software after the wound healing assay. The percentage of the wound healing was calculated as the largest migration distance (the shortest width of the wound at 0 h—the shortest width of the wound at 12 h/the width of the wound at 0 h) and the closure rate (the area of the wound at 0 h—the area of the wound at 12 h/the area of the wound at 0 h).
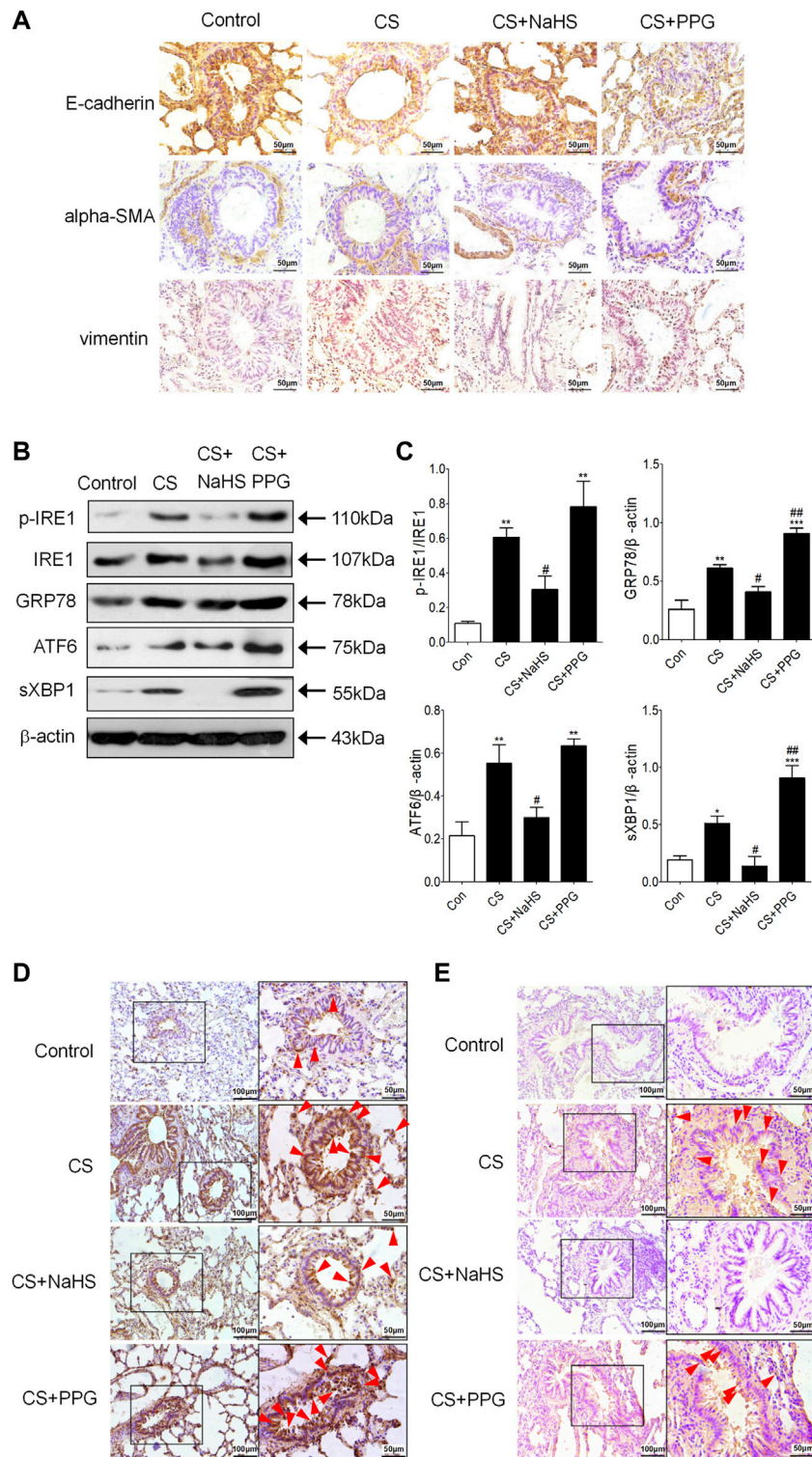
FIGURE 3 | Endogenous H₂S protects against EMT and ER stress in the lung tissues of CS-exposed rats. **(A)** E-cadherin is localized to the respiratory epithelial cell. Compared with the control group, E-cadherin was lighter in the CS group and the PPG + CS group. The NaHS + CS group had more intense E-cadherin compared with the CS group. Alpha-SMA is localized in the cytoplasm of mesenchymal cells, and Vimentin is localized in the cytoplasm of mesenchymal cells and epithelial cells. Compared with the control group, alpha-SMA and Vimentin were more intense in the CS group and the PPG + CS group, especially in bronchial epithelial cells. The NaHS + CS group had lighter alpha-SMA and Vimentin compared with the CS group. **(B,C)** Western blotting analysis of ER stresses markers p-IRE1, GRP78, ATF6 and sec-XBP1 protein expression in the lung homogenates of rats. Results are presented of 3 independent experiments ($n = 3$). Values are expressed as mean ± SEM. *$p <$
(*Continued*)

FIGURE 3 | 0.05, **$p < 0.01$ vs. control group and #$p < 0.05$ vs. CS group. **(D)** GRP78 (red arrow) is localized in the cytoplasm of respiratory epithelial cells and mesenchymal cells, especially the bronchial epithelial cells. Compared with the control group, GRP78 positive staining in the lung tissues of the CS group was significantly increased, characterized by plenty of brown granules. Compared with the CS group, GRP78 positive staining in the lung tissues of NaHS + CS group was significantly decreased, and GRP78 positive staining in the lung tissues of PPG + CS group was increased. **(E)** P-IRE1 (red arrow) is localized to the cytoplasm of respiratory epithelial cells and mesenchymal cells. Compared with control group, p-IRE1 positive staining in the lung tissues of the CS group was significantly increased, characterized by a plenty of brown granules. Compared with CS group, p-IRE1 positive staining in the lung tissues of the NaHS + CS group was significantly decreased, and p-IRE1 positive staining in the lung tissues of the PPG + CS group was increased. Representative images ($n = 4$, respectively, in each group). Original magnification ×100 and ×400.

Statistical Analysis

The data is expressed as mean ± SD (for normally distributed data) or median (for non-normally distributed data). For normally distributed data, comparisons among more than 2 groups were analyzed by one-way analysis of variance followed by the Student-Newman-Keuls test. For non-normally distributed data, the Wilcoxon signed rank test was used. $p < 0.05$ was considered statistically significant.

RESULTS

The Expression and Localization of Epithelial Mesenchymal Transition Markers and Endoplasmic Reticulum Stress Markers in Human Lung Tissues

Human peripheral lung tissues were obtained from 21 patients, including 7 smokers with COPD, 7 non-COPD smokers who had normal lung function, and 7 non-smokers who had never smoked. The average age of participants was 65.62 years old. There was no difference in age and weight among the three groups. The smoking index did not differ between non-COPD smokers and smokers with COPD. Forced expiratory volume in the first second/forced vital capacity (FEV$_1$/FVC) and FEV$_1$% were significantly lower in smokers with COPD compared with non-COPD smokers and non-smokers (**Supplementary Table S1**).

The epithelial cell markers E-cadherin and ZO-1 were decreased and the mesenchymal phenotypic marker alpha-SMA was increased in the lung tissues of smokers and COPD patients compared to non-smokers (**Figures 1A,B**). Immunohistochemistry showed that E-cadherin was located in bronchial and alveolar epithelial cells. It was strongly stained in non-smokers and decreased in non-COPD smokers and smokers with COPD (**Figure 1C**). P-IRE1 and GRP78 were increased in the lung tissue of non-COPD smokers and smokers with COPD compared with non-smokers (**Figures 1D,E**). Immunohistochemistry showed that p-IRE1 was expressed in lung epithelial cells and smooth muscle cells. It was stronger in stained non-COPD smokers and smokers with COPD compared with non-smokers (**Figure 1F**).

H$_2$S Alleviated Chronic Cigarette Smoke Exposure Induced Lung Pathological Damage and Small Airway Fibrosis

A western blot showed the protein level of CSE significantly decreased in the lung tissue of the PPG + CS group compared with the other three groups. There was no significant difference in

CSE protein expression between control, CS, and NaHS + CS groups (**Supplementary Figure S1**).

Our previous study found that the NaHS + CS and NaHS alone groups showed increased plasma H$_2$S levels than the control group. Whereas, the PPG + CS group showed a decreased plasma level of H$_2$S compared to the CS-alone group. The CS group showed higher CSE protein expression in lung tissue and plasma H$_2$S levels as compared to the control group. However, there was no significant difference in the level of H$_2$S in rat lung tissue in groups (Chen et al., 2011).

HE staining and the pathological scores of small airways showed that compared with the control group, the lung tissue of passive smoking rats showed pathological damage. Compared with CS alone, the PPG + CS group showed more severe pathological damage to lung tissue, and the NaHS + CS group showed milder pathological damage to lung tissue (**Figures 2A,B**). The degree of small airway fibrosis (collagen I and III) as determined by the Piscosirius-red polarization method was significantly higher in the COPD rat model established by passive smoking exposure. Intraperitoneal injection of NaHS in the NaHS + CS group significantly alleviated small airway fibrosis compared with CS alone, while intraperitoneal injection of PPG in the PPG + CS group exacerbated small airway fibrosis compared with CS alone (**Figures 2C,D**).

Endogenous H$_2$S Inhibited CS-Induced Lung Epithelial Cell Epithelial Mesenchymal Transition in Rats

Immunohistochemistry showed that E-cadherin was decreased in the CS group and the PPG + CS group compared with the control group. The NaHS + CS group had more intense E-cadherin compared with the CS group. Vimentin and alpha-SMA are localized mainly in the cytoplasm of mesenchymal cells. Compared with the control group, alpha-SMA and Vimentin were more intense in the CS group and the PPG + CS group, especially in bronchial epithelial cells. The NaHS + CS group had decreased alpha-SMA and Vimentin compared with the CS group (**Figure 3A**).

Endogenous H$_2$S Inhibited CS-Induced Lung Epithelial Cell Endoplasmic Reticulum Stress in Rats

Western blot showed the ER stress markers p-IRE1, GRP94, ATF6 and sec-XBP1 were increased in the lung tissue of the CS group compared with the control group. Intraperitoneal injection of NaHS in the NaHS + CS group significantly decreased these
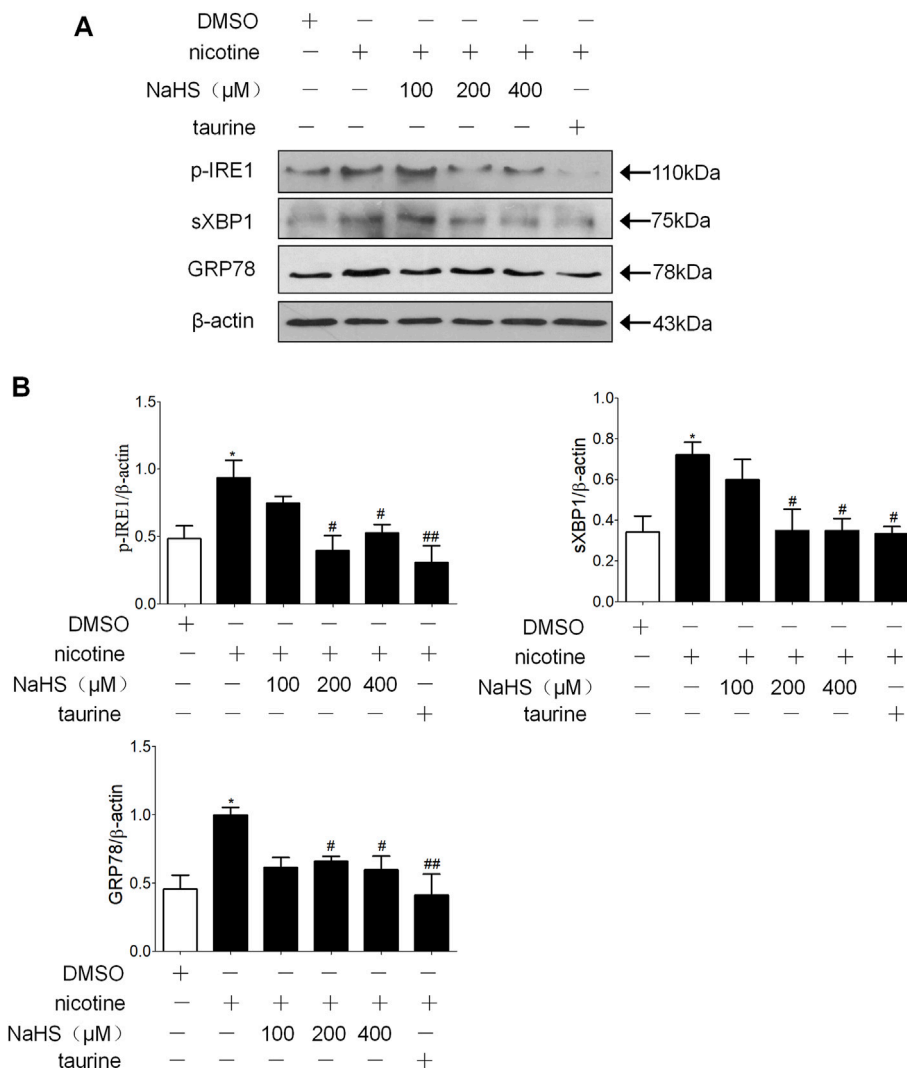
FIGURE 4 | H₂S and ER stress inhibitor taurine suppressed nicotine-induced ER stress in 16 HBE cells. **(A,B)** Nicotine (40 µmol/L) was used. Western blotting analysis of ER stress markers p-IRE1, sec-XBP1, and GRP78 protein expression in 16HBE cells, and relative intensity normalized to the expression of β-actin ($n = 3$, respectively, in each group). Values are expressed as mean ± SEM. *$p < 0.05$ vs. the DMSO group. #$p < 0.05$, ##$p < 0.01$ vs. nicotine group.

markers compared with the CS group (**Figures 3B,C**). Meanwhile, intraperitoneal injection of PPG in the PPG + CS group increased these markers compared with the CS group (**Figures 3B,C**). Immunohistochemistry showed that GRP78 was expressed mainly in lung epithelial cells, and p-IRE1 was expressed in lung epithelial cells and smooth muscle cells. They were all strongly stained in the CS group and the PPG + CS group, and lightly stained in the control group and the NaHS + CS group (**Figures 3D,E**).

H₂S Inhibited Nicotine-Induced Endoplasmic Reticulum Stress in Human Bronchial Epithelial Cells *In vitro*

Because no standard methods for the preparation of cigarette smoke extract have been established and nicotine, as an important component of cigarette smoke extract, can directly induce EMT (Dasgupta et al., 2009; Pillai et al., 2015; Zhang et al., 2016; Du et al., 2018) and ER stress (Lin et al., 2017) in the lung, we employed a pure nicotine cell model for the mechanistic work. Nicotine concentration dependently increased the expression of ER stress markers and alpha-SMA, and nicotine also concentration dependently decreased E-cadherin in 16HBE cells (**Supplementary Figure S2**). And it has been reported in our previous study that nicotine also time-dependently increased the protein level of the ER stress marker (Lin et al., 2017). 40 µmol/L nicotine treated for 72 h significantly induced ER stress and EMT in 16HBE cells.

Preincubation of 16HBE cells with NaHS and then treating them with nicotine resulted in a concentration-related inhibition of ER stress markers p-IRE1, sec-XBP1 and GRP78 formation compared with nicotine alone, appropriate concentration of
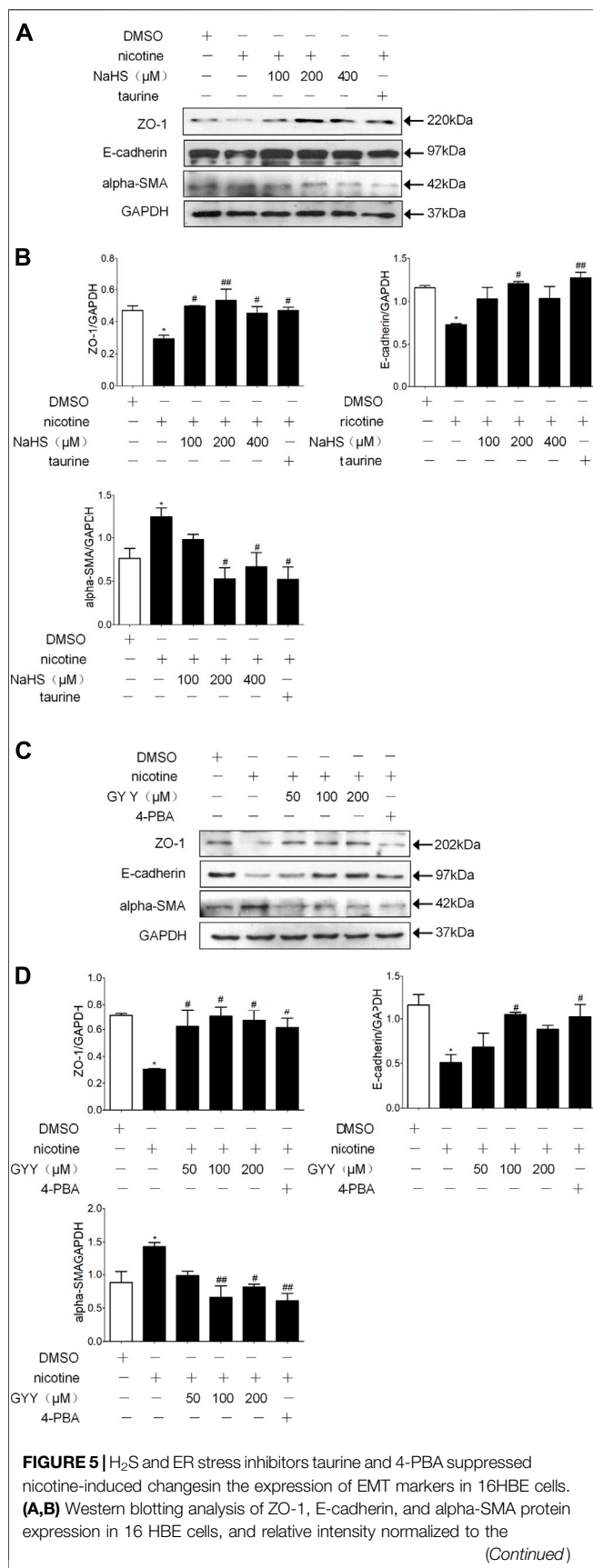
A

DMSO	+	—	—	—	—
nicotine	—	+	+	+	—	+
NaHS（μM）	—	—	100	200	400	—
taurine	—	—	—	—	—	+

ZO-1 ← 220kDa
E-cadherin ← 97kDa
alpha-SMA ← 42kDa
GAPDH ← 37kDa

B

C

DMSO	+	—	—	—	—
nicotine	—	+	+	+	+
GYY（μM）	—	—	50	100	200	—
4-PBA	—	—	—	—	—	+

ZO-1 ← 202kDa
E-cadherin ← 97kDa
alpha-SMA ← 42kDa
GAPDH ← 37kDa

D

FIGURE 5 | H₂S and ER stress inhibitors taurine and 4-PBA suppressed nicotine-induced changes in the expression of EMT markers in 16HBE cells. **(A,B)** Western blotting analysis of ZO-1, E-cadherin, and alpha-SMA protein expression in 16 HBE cells, and relative intensity normalized to the

(Continued)

FIGURE 5 | expression of GAPDH (n = 3, respectively, in each group). 200 μmol/L NaHS reversed nicotine induced-EMT to the greatest extent. Values are expressed as mean ± SEM. *p < 0.05 vs. the DMSO group. #p < 0.05, ##p < 0.01 vs. nicotine group. **(C,D)** Western blotting analysis of ZO-1, E-cadherin, and alpha-SMA protein expression in 16HBE cells, and relative intensity normalized to the expression of GAPDH (n = 3, respectively, in each group). 100 μmol/L GYY4137 reversed nicotine induced-EMT to the greatest extent. Values are expressed as mean ± SEM. *p < 0.05 vs. the DMSO group. #p < 0.05, ##p < 0.01 vs. nicotine group.

NaHS (200 μM) reduced p-IRE1, sec-XBP1 and GRP78 formation to the greatest extent (**Figures 4A,B**).

H₂S Inhibited Nicotine-Induced Human Bronchial Epithelial Cell Epithelial Mesenchymal Transition by Regulating Endoplasmic Reticulum Stress *In vitro*
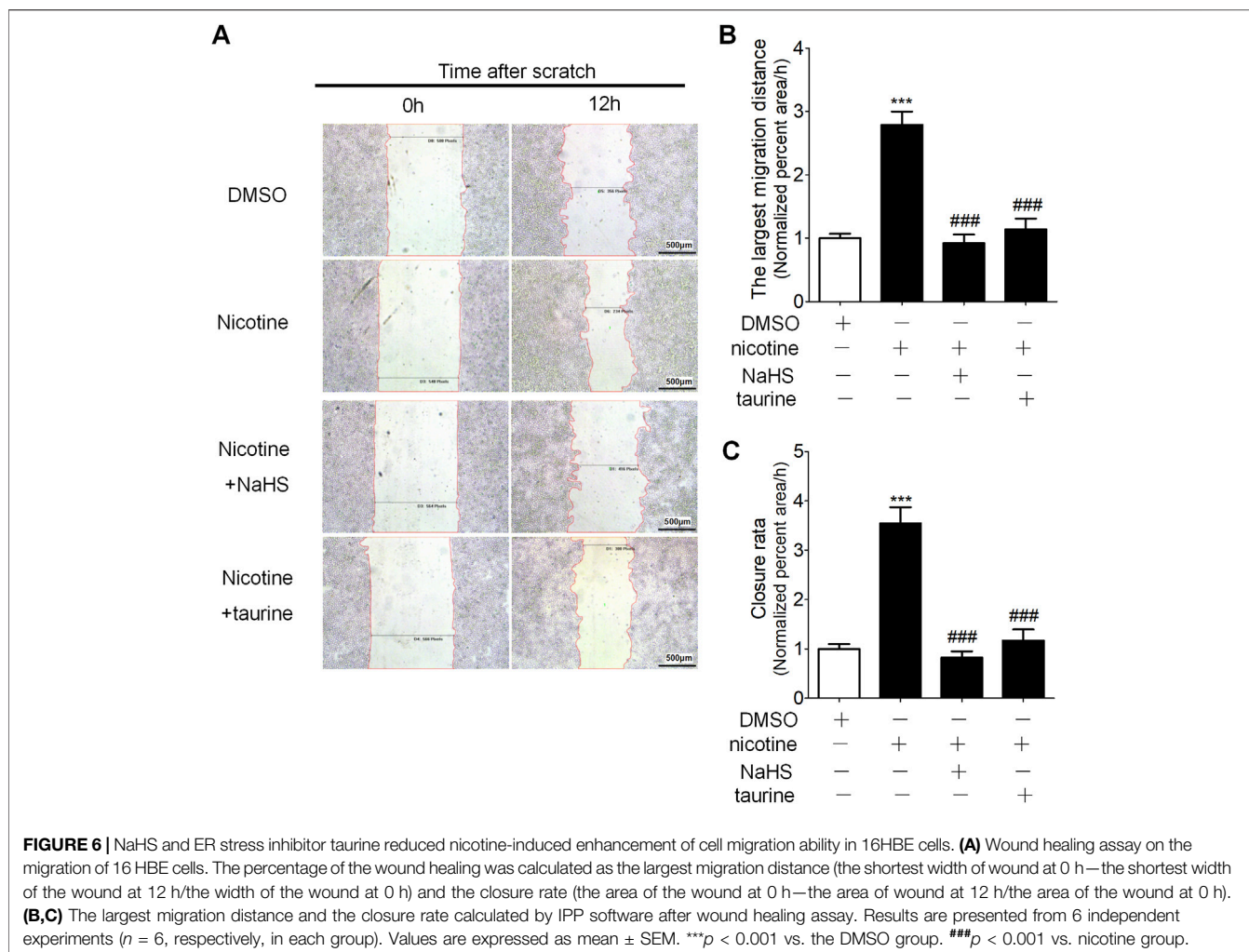
Preincubation of 16 HBE cells with H₂S donor NaHS or GYY4137 and then treating with nicotine resulted in a concentration-related down regulation of alpha-SMA and up regulation of ZO-1 and E-cadherin compared with nicotine alone. An appropriate concentration of NaHS (200 μM) reduced the expression of alpha-SMA and increased the expression of ZO-1 and E-cadherin to the greatest extent (**Figures 5A,B**). Appropriate concentration of GYY4137 (100 μM) reduced the expression of alpha-SMA and increased and the expression of E-cadherin to the greatest extent (**Figures 5C,D**). Pre-exposure 16HBE cells to ER stress inhibitor taurine or 4PBA all significantly reduced alpha-SMA expression and increased ZO-1 and E-cadherin expression (**Figure 5**).

H₂S Inhibited Nicotine-Induced Enhancement of the Migration Ability of Human Bronchial Epithelial Cells by Regulating ER Stress *In vitro*

Wound healing assay showed nicotine stimulation promoted cell migration of 16HBE cells, and preincubation of 16HBE cells with taurine or NaHS significantly retarded cell migration compared with nicotine alone (**Figure 6**).

H₂S Inhibited Human Bronchial Epithelial Cell Epithelial Mesenchymal Transition *via* Suppressing IRE1 Signal Pathway and the Activation of Smad2/3

IRE1 activation inhibitor 4μ8C decreased the phosphorylation of IRE1 and increased the protein expression level of E-cadherin compared with nicotine alone in a concentration-dependent manner (**Figures 7A,B**). The 200 μM NaHS or 6 μM 4μ8C preincubation of the 16HBE cells significantly reduced the formation of p-JNK and p-Smad2/3 (**Figures 7C,D**). Prolonged ER stress increases the phosphorylation of IRE1, which increases the phosphorylation of JNK, in our research, 6 μM 4μ8C or 200 μM NaHS inhibited nicotine-induced the activation of IRE1-JNK pathway and Smad2/3.

FIGURE 6 | NaHS and ER stress inhibitor taurine reduced nicotine-induced enhancement of cell migration ability in 16HBE cells. **(A)** Wound healing assay on the migration of 16 HBE cells. The percentage of the wound healing was calculated as the largest migration distance (the shortest width of wound at 0 h—the shortest width of the wound at 12 h/the width of the wound at 0 h) and the closure rate (the area of the wound at 0 h—the area of wound at 12 h/the area of the wound at 0 h). **(B,C)** The largest migration distance and the closure rate calculated by IPP software after wound healing assay. Results are presented from 6 independent experiments ($n = 6$, respectively, in each group). Values are expressed as mean ± SEM. ***$p < 0.001$ vs. the DMSO group. ###$p < 0.001$ vs. nicotine group.

DISCUSSION

The peripheral airways are the most vulnerable areas of the respiratory tract to CS, pollutants, and toxic substances. Therefore, inflammation, injury, and differentiation pathological changes are more common in the peripheral airways (Higham et al., 2019). Recently, a large-scale epidemiological research of 50,479 adults in China reported that the small-airways dysfunction associated to the presence of COPD (Xiao et al., 2020). Small-airways, dysfunction preceded both the detection of emphysema by imaging methods and spirometric evidence of COPD (Hogg et al., 2004). CS induced EMT in lung epithelial cells can contribute to COPD remodeling events (Sohal et al., 2010; Liu et al., 2010; Sohal et al., 2011; Veljkovic et al., 2011; Eurlings et al., 2014). The results that were found in this research showed EMT occurred in non-COPD smokers' and COPD patients' lung epithelial cells, especially in the bronchial epithelial cells (**Figure 1**). We got a similar result to the previous studies (Sohal et al., 2010) that showed EMT was indeed active in smokers' airways, in particular in the airways of smokers with COPD. EMT markers significantly correlated with

pulmonary function in COPD patients (Takizawa et al., 2001; Sohal et al., 2010). EMT markers significantly elevated in non-COPD smokers implies that EMT may be involved in the occurrence of COPD. But it still needs further work to investigate the specific connection, especially the signal pathway, between EMT and COPD, and there is a lack of an effective drug to reverse EMT and the occurrence and development of COPD.

H₂S has been confirmed to play a protective role in tissue damage in the lungs, heart, brain, gastrointestinal tract, liver, and other organs caused by a variety of stressors. According to our previous research, the level of H₂S in serum was significantly higher in non-smokers compared with smokers, and it was significantly higher in smokers with stable COPD and healthy smokers than in smoking patients who suffer from acute exacerbations of COPD (Chen et al., 2005). We also identified that H₂S significantly alleviated CS-induced lung pathological damage and lung function damage. Exogenous H₂S reduced the pathology scores of lung tissue and was antioxidant and anti-inflammatory (Chen et al., 2011). The results that were found in this research showed exogenous administration of NaHS in a
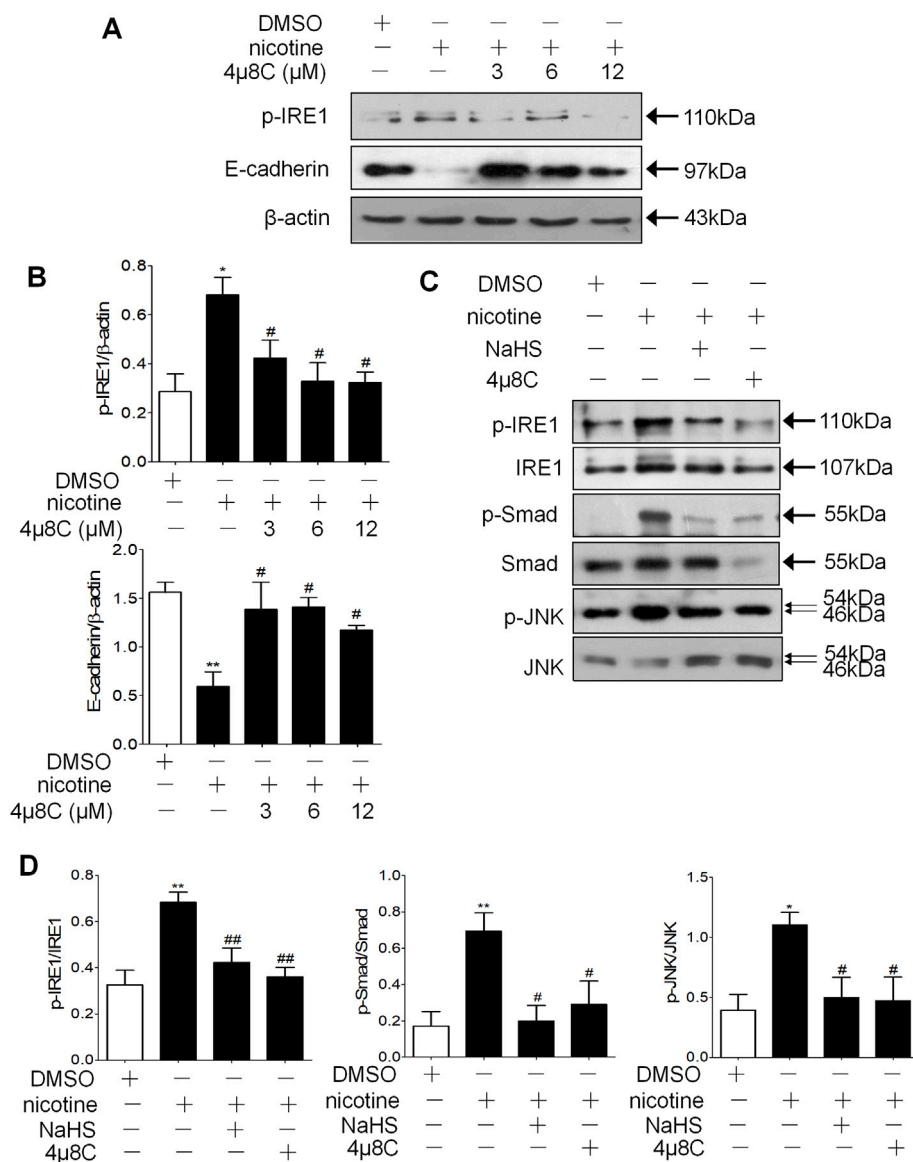
FIGURE 7 | NaHS and IRE1 activation inhibitor 4μ8C inhibited the phosphorylation of IRE1 and Smad2/3 to inhibit EMT in 16HBE cells. **(A,B)** Western blotting analysis of p-IRE1 and E-cadherin protein expression in 16HBE cells, and relative intensity normalized to the expression of β-actin ($n = 3$, respectively, in each group). Values are expressed as mean ± SEM. *$p < 0.05$ vs. the DMSO group and #$p < 0.05$ vs. nicotine group. **(C,D)** Western blotting analysis of the ratio of p-IRE1/IRE1, p-Smad2/3/Smad2/3 and p-JNK/JNK in 16HBE cells. Results are presented from 3 independent experiments ($n = 3$, respectively, in each group). Values are expressed as mean ± SEM. *$p < 0.05$, **$p < 0.01$ vs. the DMSO group. #$p < 0.05$, ##$p < 0.01$ vs. nicotine group.

COPD rat model established by passive smoking exposure significantly reversed the pathological damage in lung tissue and small airway fibrosis, whereas exogenous administration of PPG aggravated lung tissue damage and small airway fibrosis, so the endogenous H₂S played an inhibitory effect on small airway fibrosis (**Figure 2**).

Inhibition of endogenous H₂S by CSE inhibitor PPG resulted in EMT-like features, increased the protein expression of vimentin and decreased the protein expression of E-cadherin. Exogenous administration of H₂S decreased these effects in the non-small cell lung cancer cell line A549 stimulated by TGF-β1

(Fang et al., 2010). In our previous research, H₂S inhibited EMT occurrence in human bronchial epithelial cell line 16HBE induced by TGF-β1 (Liao et al., 2015). The results that were found in this research showed exogenous administration of NaHS in the COPD rat model established by passive smoking exposure significantly reversed EMT, whereas intraperitoneal injection of PPG aggravated EMT in lung epithelial cells (**Figure 3**). This is consistent with the trend of small airway fibrosis in these groups. These results suggest that in lung epithelial cells, endogenous H₂S may have an inhibitory effect on EMT related small airway fibrosis.

It has been confirmed that the main mutagenicity components of CS condensates exist in alkaline and slightly acidic parts, while the mutagenicity was not detected in neutral parts containing polycyclic aromatic hydrocarbons (Kier et al., 1974; Hutton and Hackney, 1975). It suggests that mutagenic components in CS condensates mainly exist in the water-soluble part, and the water-soluble part of CS is more easily dissolved and absorbed by the mucus on the alveolar surface (Ji and Chen, 1996). Acrolein, nicotine, and acetylaldehyde are among the most important and relevant chemicals in CS (Comer et al., 2014). Acrolein is highly toxic, a large number of studies have shown that acrolein can induce apoptosis (Kern and Kehrer, 2002; Roy et al., 2010), but few studies have shown that it can induce EMT and ER stress. When tobacco smoke reaches the small airways and alveolar surface, the nicotine is rapidly absorbed. On average, about 1–0.5 mg of nicotine is absorbed systemically during smoking on average (Benowitz and Iii, 1984). Nicotine is directly associated with COPD. Evaluation of electronic nicotine delivery systems in different models has demonstrated involvement in pathways related to chronic pulmonary diseases (Canistro et al., 2017; Singh et al., 2019; Mikheev et al., 2020). Inhaled nicotine induced bronchial epithelial cell senescence and apoptosis *via* ROS-mediated autophagy impairment in COPD patients (Bodas et al., 2016). Nicotine can promote EMT in the lungs. Maternal nicotine exposure induces EMT in rat offspring lungs (Chen et al., 2015). Nicotine can increase malignancy through EMT in lung cancer (Dasgupta et al., 2009; Pillai et al., 2015; Zhang et al., 2016; Du et al., 2018). Nicotine can directly induce ER stress response (Pelissier-Rota et al., 2015; Barra et al., 2017; Gonzales et al., 2021; Jiang et al., 2021). In our previous study, we used a nicotine exposure model to investigate whether H₂S can inhibit cigarette smoke-induced ERS and apoptosis in bronchial epithelial cells (Lin et al., 2017). Our previous study confirmed that nicotine concentration and time-dependently increased the expression of ER stress associated apoptosis marker in human bronchial epithelial cells, participating in the progression of COPD (Lin et al., 2017).

ER stress can activate classic Smad, Wnt/β-catenin and Src protein kinase families, thus inducing EMT in alveolar epithelial cells (Tanjore et al., 2011; Zhong et al., 2011; Zhang et al., 2012) ER stress participates in EMT and oncogenesis (Sheshadri et al., 2014). The results that were found in this research showed H₂S inhibited lung epithelial cell ER stress and EMT in a COPD rat model established by passive smoking exposure (**Figure 3**). In the 16HBE cells exposed to nicotine, a suitable concentration of GYY4137 or NaHS not only inhibited nicotine-induced ER stress, but also inhibited nicotine-induced enhancement of cell migration ability and EMT (**Figure 5**). ER stress nonspecific inhibitor taurine or 4-PBA also suppressed the enhancement of cell migration ability and EMT in 16HBE cells exposed to nicotine (**Figure 6**). A suitable concentration of H₂S can simulate this effect. The results shown above indicate that H₂S can inhibit EMT through regulating ER stress.

We also investigated the signaling pathways of ER stress to influence the occurrence of EMT in bronchial epithelial cells by H₂S. We found that the inhibition of IRE1 signaling pathways significantly alleviated the nicotine-induced down-regulated expression of E-cadherin (**Figure 7**). This finding is supported by a previous report of alveolar epithelial cells (Zhong et al., 2011), which suggests that inhibition of IRE1 signaling pathways can reverse EMT. Furthermore, we identified that both 4μ8C and H₂S suppressed the activation of IRE1, Smad2/3, and JNK (**Figure 7**). Excessive ER stress results in kinase activity of IRE1 along with phosphorylation of JNK. In our research, H₂S and 4μ8C inhibited nicotine-induced IRE1 kinase activation, thus inhibiting the activation of IRE1 downstream signal molecules including JNK and Smad2/3. Our finding is supported by previous reports of alveolar epithelial cells (Zhong et al., 2011), which suggest that p-IRE1 and EMT-related signal molecule Smad2/3 play an essential role in EMT mediated by ER stress, and pretreatment of H₂S suppressed the phosphorylation of Smad2/3 stimulated by TGF-β1. Both Smad2/3 inhibitor and H₂S could inhibit ER stress-induced EMT (41). In this research, we identified that H₂S could inhibit bronchial epithelial cell EMT through suppressing the activation of IRE1 and its downstream signal molecule Smad2/3. Our finding suggested that H₂S could also inhibit ATF6 activation. Another report reported that activation of PERK and ATF can cause EMT (Sheshadri et al., 2014). Therefore, it is not clear that H₂S can directly act on IRE1 or regulate the upstream signal pathway of ER stress. According to recent reports, H₂S can regulate ER stress in different organ systems through different action sites. H₂S can directly persulfidate protein kinase and regulate the protein kinase activity (Du et al., 2021). H₂S may reduce ER stress via regulation of Ca²⁺ channel sulfhydration (Hennig and Diener, 2009; Luciani et al., 2009; Moccia et al., 2011). H₂S may regulate ER stress through its antioxidant effect. Some studies have revealed that H₂S can both regulate oxidative stress and ER stress (Hu et al., 2017; Majumder et al., 2018; Yi et al., 2018). In addition, H₂S can inhibit homocysteine-induced neurocyte ER stress and apoptosis by up-regulation of the brain-derived neurotrophic factor (BDNF)-TrkB pathway (Wei et al., 2014). Our research identified that H₂S significantly inhibiting CS-induced ER stress, thus inhibited ER stress-mediated EMT.

There are several limitations to our investigation. Firstly, we have not figured out the specific signal pathway of H₂S on ER stress. Knock out the gene in the IRE1 signal pathway or Smad2/3 may be a better way to figure out the importance of these signal molecules in ER stress mediated EMT. Secondly, the number of lung tissue samples was too small. We are ready to recruit more patients, including non-smoking COPD patients and COPD patients in different GOLD stages, in the future study. Immunofluorescence staining and co-staining with EMT marker and ER stress marker is a better way than immunohistochemical staining to identify the cells that undergo EMT and ER stress. Further studies are needed to overcome these shortcomings.

In conclusion, it is proved for the first time that H₂S can inhibit CS- or nicotine-induced ER stress and EMT in bronchial epithelial cells. The IRE1 signal pathway and its downstream signal molecule p-Smad2/3 may be responsible for the inhibitory

effect of H₂S. These findings suggest a possible protective role of anti-fibrosis for H₂S in the pathogenesis of COPD.

DATA AVAILABILITY STATEMENT

The raw data supporting the conclusion of this article will be made available by the authors, without undue reservation.

ETHICS STATEMENT

The studies involving human participants were reviewed and approved by the protocol was approved by the Ethics Committee of Peking University Third Hospital, approval number IRB00006761-2012029. The patients/participants provided their written informed consent to participate in this study. The animal study was reviewed and approved by all animal care and experimental protocols were in compliance with the ethical procedures and policies approved by the Animal Care and Use Committee of the National Research Center and the Third Hospital, Peking University Guide for the Care and Use of Laboratory Animals.

AUTHOR CONTRIBUTIONS

FL optimized techniques, performed the experiments, and was involved in writing the manuscript. CL, JZ, YS, WL, YB, YL, and ML were involved in developing some of the methods. YQ and YC designed and guided the experiments and revised the manuscript.

SUPPLEMENTARY MATERIAL

The Supplementary Material for this article can be found online at: https://www.frontiersin.org/articles/10.3389/fmolb.2022.828766/full#supplementary-material

REFERENCES

Alam, S., Li, Z., Atkinson, C., Jonigk, D., Janciauskiene, S., and Mahadeva, R. (2014). Z α1-Antitrypsin Confers a Proinflammatory Phenotype that Contributes to Chronic Obstructive Pulmonary Disease. *Am. J. Respir. Crit. Care Med.* 189, 909–931. doi:10.1164/rccm.201308-1458OC

Barra, N. G., Lisyansky, M., Vanduzer, T. A., Raha, S., Holloway, A. C., and Hardy, D. B. (2017). Maternal Nicotine Exposure Leads to Decreased Cardiac Protein Disulfide Isomerase and Impaired Mitochondrial Function in Male Rat Offspring. *J. Appl. Toxicol.* 37, 1517–1526. doi:10.1002/jat.3503

Benowitz, N. L., and Iii, P. J., 3rd (1984). Daily Intake of Nicotine during Cigarette Smoking. *Clin. Pharmacol. Ther.* 35, 499–504. doi:10.1038/clpt.1984.67

Bodas, M., Van Westphal, C., Carpenter-Thompson, R., K. Mohanty, D. N., and Vij, N. (2016). Nicotine Exposure Induces Bronchial Epithelial Cell Apoptosis and Senescence via ROS Mediated Autophagy-Impairment. *Free Radic. Biol. Med.* 97, 441–453. doi:10.1016/j.freeradbiomed.2016.06.017

Canistro, D., Vivarelli, F., Cirillo, S., Babot Marquillas, C., Buschini, A., Lazzaretti, M., et al. (2017). E-cigarettes Induce Toxicological Effects that Can Raise the Cancer Risk. *Sci. Rep.* 7, 2028. doi:10.1038/s41598-017-02317-8

Chadwick, S. R., and Lajoie, P. (2019). Endoplasmic Reticulum Stress Coping Mechanisms and Lifespan Regulation in Health and Diseases. *Front. Cel Dev. Biol.* 7, 84. doi:10.3389/fcell.2019.00084

Chen, C.-M., Chou, H.-C., and Huang, L.-T. (2015). Maternal Nicotine Exposure Induces Epithelial-Mesenchymal Transition in Rat Offspring Lungs. *Neonatology* 108, 179–187. doi:10.1159/000437012

Chen, Y.-H., Wang, P.-P., Wang, X.-M., He, Y.-J., Yao, W.-Z., Qi, Y.-F., et al. (2011). Involvement of Endogenous Hydrogen Sulfide in Cigarette Smoke-Induced Changes in Airway Responsiveness and Inflammation of Rat Lung. *Cytokine* 53, 334–341. doi:10.1016/j.cyto.2010.12.006

Chen, Y.-H., Yao, W.-Z., Geng, B., Ding, Y.-L., Lu, M., Zhao, M.-W., et al. (2005). Endogenous Hydrogen Sulfide in Patients with COPD. *Chest* 128, 3205–3211. doi:10.1378/chest.128.5.3205

Comer, D. M., Elborn, J. S., and Ennis, M. (2014). Inflammatory and Cytotoxic Effects of Acrolein, Nicotine, Acetylaldehyde and Cigarette Smoke Extract on Human Nasal Epithelial Cells. *BMC Pulm. Med.* 14, 32. doi:10.1186/1471-2466-14-32

Cosio, M., Ghezzo, H., Hogg, J. C., Corbin, R., Loveland, M., Dosman, J., et al. (1978). The Relations between Structural Changes in Small Airways and Pulmonary-Function Tests. *N. Engl. J. Med.* 298, 1277–1281. doi:10.1056/NEJM197806082982303

Dasgupta, P., Rizwani, W., Pillai, S., Kinkade, R., Kovacs, M., Rastogi, S., et al. (2009). Nicotine Induces Cell Proliferation, Invasion and Epithelial-Mesenchymal Transition in a Variety of Human Cancer Cell Lines. *Int. J. Cancer* 124, 36–45. doi:10.1002/ijc.23894

Du, X., Jin, Z., Liu, Z., Liu, D., Zhang, L., Ma, X., et al. (2021). H2S Persulfidated and Increased Kinase Activity of MPK4 to Response Cold Stress in Arabidopsis. *Front. Mol. Biosci.* 8, 635470. doi:10.3389/fmolb.2021.635470

Du, X., Qi, F., Lu, S., Li, Y., and Han, W. (2018). Nicotine Upregulates FGFR3 and RB1 Expression and Promotes Non-small Cell Lung Cancer Cell Proliferation and Epithelial-To-Mesenchymal Transition via Downregulation of miR-99b and miR-192. *Biomed. Pharmacother.* 101, 656–662. doi:10.1016/j.biopha.2018.02.113

Eurlings, I. M. J., Reynaert, N. L., van den Beucken, T., Gosker, H. R., de Theije, C. C., Verhamme, F. M., et al. (2014). Cigarette Smoke Extract Induces a Phenotypic Shift in Epithelial Cells; Involvement of HIF1α in Mesenchymal Transition. *PLoS One* 9, e107757. doi:10.1371/journal.pone.0107757

Fang, L.-P., Lin, Q., Tang, C.-S., and Liu, X.-M. (2010). Hydrogen Sulfide Attenuates Epithelial-Mesenchymal Transition of Human Alveolar Epithelial Cells. *Pharmacol. Res.* 61, 298–305. doi:10.1016/j.phrs.2009.10.008

Geraghty, P., Baumlin, N., Salathe, M. A., Foronjy, R. F., and D'Armiento, J. M. (2016). Glutathione Peroxidase-1 Suppresses the Unfolded Protein Response upon Cigarette Smoke Exposure. *Mediators Inflamm.* 2016, 1–16. doi:10.1155/2016/9461289

GOLD (Global Initiative for Chronic Obstructive Lung Disease) (2009). Global Strategy for the Diagnosis, Management, and Prevention of Chronic Obstructive Pulmonary Disease. Available from: http://wwwgoldcopdorg/guidelines-global-strategy-for-diagnosis-managementhtml.

Gonzales, K., Feng, V., Bikkina, P., Landicho, M. A., Haas, M. J., and Mooradian, A. D. (2021). The Effect of Nicotine and Dextrose on Endoplasmic Reticulum Stress in Human Coronary Artery Endothelial Cells. *Toxicol. Res. (Camb)* 10, 284–291. doi:10.1093/toxres/tfab012

Guan, R., Wang, J., Cai, Z., Li, Z., Wang, L., Li, Y., et al. (2020). Hydrogen Sulfide Attenuates Cigarette Smoke-Induced Airway Remodeling by Upregulating SIRT1 Signaling Pathway. *Redox Biol.* 28, 101356. doi:10.1016/j.redox.2019.101356

Hennig, B., and Diener, M. (2009). Actions of Hydrogen Sulphide on Ion Transport across Rat Distal colon. *Br. J. Pharmacol.* 158, 1263–1275. doi:10.1111/j.1476-5381.2009.00385.x

Higham, A., Quinn, A. M., Cançado, J. E. D., and Singh, D. (2019). The Pathology of Small Airways Disease in COPD: Historical Aspects and Future Directions. *Respir. Res.* 20, 49. doi:10.1186/s12931-019-1017-y

Hogg, J. C., Chu, F., Utokaparch, S., Woods, R., Elliott, W. M., Buzatu, L., et al. (2004). The Nature of Small-Airway Obstruction in Chronic Obstructive Pulmonary Disease. *N. Engl. J. Med.* 350, 2645–2653. doi:10.1056/NEJMoa032158

Hu, H.-J., Jiang, Z.-S., Qiu, J., Zhou, S.-H., and Liu, Q.-M. (2017). Protective Effects of Hydrogen Sulfide against Angiotensin II-Induced Endoplasmic Reticulum Stress in HUVECs. *Mol. Med. Rep.* 15, 2213–2222. doi:10.3892/mmr.2017.6238

Hutton, J. J., and Hackney, C. (1975). Metabolism of Cigarette Smoke Condensates by Human and Rat Homogenates to Form Mutagens Detectable by *Salmonella typhimurium* TA1538. *Cancer Res.* 35, 2461–2468.

Ji, Q., and Chen, Y. (1996). Vicia faba Root Tip Micronucleus Test on the Mutagenicity of Water-Soluble Contents of Cigarette Smoke. *Mutat. Research/Environmental Mutagenesis Relat. Subjects* 359, 1–6. doi:10.1016/s0165-1161(96)90003-5

Jiang, Y. J., Cui, S., Luo, K., Ding, J., Nan, Q. Y., Piao, S. G., et al. (2021). Nicotine Exacerbates Tacrolimus-Induced Renal Injury by Programmed Cell Death. *Korean J. Intern. Med.* 36, 1437–1449. doi:10.3904/kjim.2021.326

Kern, J. C., and Kehrer, J. P. (2002). Acrolein-induced Cell Death: a Caspase-Influenced Decision between Apoptosis and Oncosis/necrosis. *Chemico-Biological Interactions* 139, 79–95. doi:10.1016/s0009-2797(01)00295-2

Kier, L. D., Yamasaki, E., and Ames, B. N. (1974). Detection of Mutagenic Activity in Cigarette Smoke Condensates. *Proc. Natl. Acad. Sci. U.S.A.* 71, 4159–4163. doi:10.1073/pnas.71.10.4159

Liang, C.-C., Park, A. Y., and Guan, J.-L. (2007). *In Vitro* scratch Assay: a Convenient and Inexpensive Method for Analysis of Cell Migration *In Vitro*. *Nat. Protoc.* 2, 329–333. doi:10.1038/nprot.2007.30

Liao, C.-C., Chen, Y.-H., Lin, F., and Qi, Y.-F. (2015). Hydrogen Sulfide Inhibits Transforming Growth Factor Beta-1 Induced Bronchial Epithelial-Mesenchymal Transition. *Chin. Med. J. (Engl.)* 128, 3247–3250. doi:10.4103/0366-6999.170266

Lin, F., Liao, C., Sun, Y., Zhang, J., Lu, W., Bai, Y., et al. (2017). Hydrogen Sulfide Inhibits Cigarette Smoke-Induced Endoplasmic Reticulum Stress and Apoptosis in Bronchial Epithelial Cells. *Front. Pharmacol.* 8, 675. doi:10.3389/fphar.2017.00675

Lin, J. H., Walter, P., and Yen, T. S. B. (2008). Endoplasmic Reticulum Stress in Disease Pathogenesis. *Annu. Rev. Pathol. Mech. Dis.* 3, 399–425. doi:10.1146/annurev.pathmechdis.3.121806.151434

Lindholm, D., Korhonen, L., Eriksson, O., and Kõks, S. (2017). Recent Insights into the Role of Unfolded Protein Response in ER Stress in Health and Disease. *Front. Cel Dev. Biol.* 5, 48. doi:10.3389/fcell.2017.00048

Liu, Y., Gao, W., and Zhang, D. (2010). Effects of Cigarette Smoke Extract on A549 Cells and Human Lung Fibroblasts Treated with Transforming Growth Factor-B1 in a Coculture System. *Clin. Exp. Med.* 10, 159–167. doi:10.1007/s10238-009-0081-x

Luciani, D. S., Gwiazda, K. S., Yang, T.-L. B., Kalynyak, T. B., Bychkivska, Y., Frey, M. H. Z., et al. (2009). Roles of IP3R and RyR Ca2+ Channels in Endoplasmic Reticulum Stress and β-Cell Death. *Diabetes* 58, 422–432. doi:10.2337/db07-1762

Majumder, A., Singh, M., Behera, J., Theilen, N. T., George, A. K., Tyagi, N., et al. (2018). Hydrogen Sulfide Alleviates Hyperhomocysteinemia-Mediated Skeletal Muscle Atrophy via Mitigation of Oxidative and Endoplasmic Reticulum Stress Injury. *Am. J. Physiology-Cell Physiol.* 315, C609–C622. doi:10.1152/ajpcell.00147.2018

Marciniak, S. J. (2017). Endoplasmic Reticulum Stress in Lung Disease. *Eur. Respir. Rev.* 26, 170018. doi:10.1183/16000617.0018-2017

Mikheev, V. B., Buehler, S. S., Brinkman, M. C., Granville, C. A., Lane, T. E., Ivanov, A., et al. (2020). The Application of Commercially Available Mobile Cigarette Topography Devices for E-Cigarette Vaping Behavior Measurements. *Nicotine Tob. Res.* 22, 681–688. doi:10.1093/ntr/nty190

Min, T., Bodas, M., Mazur, S., and Vij, N. (2011). Critical Role of Proteostasis-Imbalance in Pathogenesis of COPD and Severe Emphysema. *J. Mol. Med.* 89, 577–593. doi:10.1007/s00109-011-0732-8

Moccia, F., Bertoni, G., Florio Pla, A., Dragoni, S., Pupo, E., Merlino, A., et al. (2011). Hydrogen Sulfide Regulates Intracellular Ca2+ Concentration in Endothelial Cells from Excised Rat Aorta. *Cpb* 12, 1416–1426. doi:10.2174/138920111798281117

Nowrin, K., Sohal, S. S., Peterson, G., Patel, R., and Walters, E. H. (2014). Epithelial-mesenchymal Transition as a Fundamental Underlying Pathogenic Process in COPD Airways: Fibrosis, Remodeling and Cancer. *Expert Rev. Respir. Med.* 8, 547–559. doi:10.1586/17476348.2014.948853

Osorio, F., Lambrecht, B., and Janssens, S. (2013). The UPR and Lung Disease. *Semin. Immunopathol* 35, 293–306. doi:10.1007/s00281-013-0368-6

Pelissier-Rota, M. A., Pelosi, L., Meresse, P., and Jacquier-Sarlin, M. R. (2015). Nicotine-induced Cellular Stresses and Autophagy in Human Cancer colon Cells: A Supportive Effect on Cell Homeostasis via Up-Regulation of Cox-2 and PGE2 Production. *Int. J. Biochem. Cel Biol.* 65, 239–256. doi:10.1016/j.biocel.2015.06.013

Pillai, S., Trevino, J., Rawal, B., Singh, S., Kovacs, M., Li, X., et al. (2015). β-Arrestin-1 Mediates Nicotine-Induced Metastasis through E2F1 Target Genes that Modulate Epithelial-Mesenchymal Transition. *Cancer Res.* 75, 1009–1020. doi:10.1158/0008-5472.CAN-14-0681

Roy, J., Pallepati, P., Bettaieb, A., and Averill-Bates, D. A. (2010). Acrolein Induces Apoptosis through the Death Receptor Pathway in A549 Lung Cells: Role of p53This Review Is One of a Selection of Papers Published in a Special Issue on Oxidative Stress in Health and Disease. *Can. J. Physiol. Pharmacol.* 88, 353–368. doi:10.1139/Y09-134

Sheshadri, N., Catanzaro, J. M., Bott, A. J., Sun, Y., Ullman, E., Chen, E. I., et al. (2014). SCCA1/SERPINB3 Promotes Oncogenesis and Epithelial-Mesenchymal Transition via the Unfolded Protein Response and IL6 Signaling. *Cancer Res.* 74, 6318–6329. doi:10.1158/0008-5472.CAN-14-0798

Singh, K. P., Lawyer, G., Muthumalage, T., Maremanda, K. P., Khan, N. A., McDonough, S. R., et al. (2019). Systemic Biomarkers in Electronic Cigarette Users: Implications for Noninvasive Assessment of Vaping-Associated Pulmonary Injuries. *ERJ Open Res.* 5, 00182–02019. doi:10.1183/23120541.00182-2019

Sohal, S. S., Reid, D., Soltani, A., Ward, C., Weston, S., Muller, H. K., et al. (2011). Evaluation of Epithelial Mesenchymal Transition in Patients with Chronic Obstructive Pulmonary Disease. *Respir. Res.* 12, 130. doi:10.1186/1465-9921-12-130

Sohal, S. S., Reid, D., Soltani, A., Ward, C., Weston, S., Muller, H. K., et al. (2010). Reticular Basement Membrane Fragmentation and Potential Epithelial Mesenchymal Transition Is Exaggerated in the Airways of Smokers with Chronic Obstructive Pulmonary Disease. *Respirology* 15, 930–938. doi:10.1111/j.1440-1843.2010.01808.x

Stockley, J. A., Ismail, A. M., Hughes, S. M., Edgar, R., Stockley, R. A., and Sapey, E. (2017). Maximal Mid-expiratory Flow Detects Early Lung Disease in α1-antitrypsin Deficiencyflow Detects Early Lung Disease in α1antitrypsin Defciency. *Eur. Respir. J.* 49, 1602055. doi:10.1183/13993003.02055-2016

Sun, Y., Wang, K., Li, M.-X., He, W., Chang, J.-R., Liao, C.-C., et al. (2015). Metabolic Changes of H2S in Smokers and Patients of COPD Which Might Involve in Inflammation, Oxidative Stress and Steroid Sensitivity. *Sci. Rep.* 5, 14971. doi:10.1038/srep14971(

Suzuki, Y., Saito, J., Munakata, M., and Shibata, Y. (2021). Hydrogen Sulfide as a Novel Biomarker of Asthma and Chronic Obstructive Pulmonary Disease. *Allergol. Int.* 70, 181–189. doi:10.1016/j.alit.2020.10.003

Tabas, I., and Ron, D. (2011). Integrating the Mechanisms of Apoptosis Induced by Endoplasmic Reticulum Stress. *Nat. Cel Biol* 13, 184–190. doi:10.1038/ncb0311-184

Takizawa, H., Tanaka, M., Takami, K., Ohtoshi, T., Ito, K., Satoh, M., et al. (2001). Increased Expression of Transforming Growth Factor- β 1 in Small Airway Epithelium from Tobacco Smokers and Patients with Chronic Obstructive Pulmonary Disease (COPD). *Am. J. Respir. Crit. Care Med.* 163, 1476–1483. doi:10.1164/ajrccm.163.6.9908135

Tanjore, H., Blackwell, T. S., and Lawson, W. E. (2012). Emerging Evidence for Endoplasmic Reticulum Stress in the Pathogenesis of Idiopathic Pulmonary Fibrosis. *Am. J. Physiology-Lung Cell Mol. Physiol.* 302, L721–L729. doi:10.1152/ajplung.00410.2011

Tanjore, H., Cheng, D.-S., Degryse, A. L., Zoz, D. F., Abdolrasulnia, R., Lawson, W. E., et al. (2011). Alveolar Epithelial Cells Undergo Epithelial-To-Mesenchymal Transition in Response to Endoplasmic Reticulum Stress. *J. Biol. Chem.* 286, 30972–30980. doi:10.1074/jbc.M110.181164

Van den Berge, M., Ten Hacken, N. H. T., Cohen, J., Douma, W. R., and Postma, D. S. (2011). Small Airway Disease in Asthma and COPD. *Chest* 139, 412–423. doi:10.1378/chest.10-1210

Veljkovic, E., Jiricny, J., Menigatti, M., Rehrauer, H., and Han, W. (2011). Chronic Exposure to Cigarette Smoke Condensate *In Vitro* Induces Epithelial to Mesenchymal Transition-like Changes in Human Bronchial Epithelial Cells, BEAS-2B. *Toxicol. Vitro* 25, 446–453. doi:10.1016/j.tiv.2010.11.011

Wang, R., Ibarra-Sunga, O., Verlinski, L., Pick, R., and Uhal, B. D. (2000). Abrogation of Bleomycin-Induced Epithelial Apoptosis and Lung Fibrosis by Captopril or by a Caspase Inhibitor. *Am. J. Physiology-Lung Cell Mol. Physiol.* 279, L143–L151. doi:10.1152/ajplung.2000.279.1.L143

Wang, R. (2002). Two's Company, Three's a Crowd: Can H2S Be the Third Endogenous Gaseous Transmitter? *FASEB j.* 16, 1792–1798. doi:10.1096/fj.02-0211hyp

Wei, H.-j., Xu, J.-h., Li, M.-h., Tang, J.-p., Zou, W., Zhang, P., et al. (2014). Hydrogen Sulfide Inhibits Homocysteine-Induced Endoplasmic Reticulum Stress and Neuronal Apoptosis in Rat hippocampus via Upregulation of the BDNF-TrkB Pathway. *Acta Pharmacol. Sin* 35, 707–715. doi:10.1038/aps.2013.197

Xiao, D., Chen, Z., Wu, S., Huang, K., Xu, J., Yang, L., et al. (2020). Prevalence and Risk Factors of Small Airway Dysfunction, and Association with Smoking, in China: Findings from a National Cross-Sectional Study. *Lancet Respir. Med.* 8, 1081–1093. doi:10.1016/S2213-2600(20)30155-7

Yi, J., Yuan, Y., Zheng, J., and Hu, N. (2018). Hydrogen Sulfide Alleviates Uranium-Induced Kidney Cell Apoptosis Mediated by ER Stress via 20S Proteasome Involving in Akt/GSK-3β/Fyn-Nrf2 Signaling. *Free Radic. Res.* 52, 1020–1029. doi:10.1080/10715762.2018.1514603

You, H., Lei, P., and Andreadis, S. T. (2013). JNK Is a Novel Regulator of Intercellular Adhesion. *Tissue Barriers* 1, e26845. doi:10.4161/tisb.26845

Zhang, C., Ding, X.-P., Zhao, Q.-N., Yang, X.-J., An, S.-M., Wang, H., et al. (2016). Role of α7-nicotinic Acetylcholine Receptor in Nicotine-Induced Invasion and Epithelial-To-Mesenchymal Transition in Human Non-small Cell Lung Cancer Cells. *Oncotarget* 7, 59199–59208. doi:10.18632/oncotarget.10498

Zhang, H., Liu, H., Borok, Z., Davies, K. J. A., Ursini, F., and Forman, H. J. (2012). Cigarette Smoke Extract Stimulates Epithelial-Mesenchymal Transition through Src Activation. *Free Radic. Biol. Med.* 52, 1437–1442. doi:10.1016/j.freeradbiomed.2012.01.024

Zhong, Q., Zhou, B., Ann, D. K., Minoo, P., Liu, Y., Banfalvi, A., et al. (2011). Role of Endoplasmic Reticulum Stress in Epithelial-Mesenchymal Transition of Alveolar Epithelial Cells. *Am. J. Respir. Cel Mol Biol* 45, 498–509. doi:10.1165/rcmb.2010-0347OC